ADVANCED ENERGY MATERIALS
www.advenergymat.de

Spontaneous Charge Transfer and Dipole Formation at the Interface Between P3HT and PCBM

*Harri Aarnio, Parisa Sehati, Slawomir Braun, Mathias Nyman, Michel P. de Jong, Mats Fahlman, and Ronald Österbacka**

In the pursuit of developing new materials for more efficient bulk-heterojunction solar cells, the blend poly (3-hexylthiophene):[6,6]-phenyl-C_{61}-butyric acid methyl ester (P3HT:PCBM) serves as an important model system. The success of the P3HT:PCBM blend comes from efficient charge generation and transport with low recombination. There is not, however, a good microscopic picture of what causes these, hindering the development of new material systems. In this report UV photoelectron spectroscopy measurements on both regiorandom- (rra) and regioregular- (rr) P3HT are presented, and the results are interpreted using the Integer Charge Transfer model. The results suggest that spontaneous charge transfer from P3HT to PCBM occurs after heat treatment of P3HT:PCBM blends. The resulting formation of an interfacial dipole creates an extra barrier at the interface explaining the reduced (non-)geminate recombination with increased charge generation in heat treated rr-P3HT:PCBM blends. Extensive photoinduced absorption measurements using both above- and below-bandgap excitation light are presented, in good agreement with the suggested dipole formation.

The bulk-heterojunction concept was originally developed to allow for a large active interfacial area between the donor and acceptor materials in organic solar cells.[1] The energy offsets between the lowest unoccupied molecular orbital (LUMO) levels of the donor and acceptor are tuned to efficiently dissociate photogenerated excitons, i.e. an offset on the order of >0.5 eV is efficiently promoting electron transfer to the acceptor and prohibiting back-transfer to the donor. However, after dissociation the charge carriers are still Coulombically bound at zero external field within the Coulomb radius $r_c = e^2/4\pi\varepsilon\varepsilon_0 kT$, where e is the electron charge, $\varepsilon(\varepsilon_0)$ is the relative (absolute) dielectric permittivity, k the Boltzmann constant and T is the temperature. The formation of a ground-state charge transfer (CT) state opens up (non-)radiative recombination channels at the interface, where the Coulombically bound carriers can eventually recombine both geminately and non-geminately, causing recombination losses in solar cells.

Recent reports on charge transfer state formation in the ground state of the polymer/fullerene mixtures suggests that the CT state arises from a wave function overlap of the polymer and fullerene molecules,[2–7] whereby a new inter-bandgap charge transfer complex state is formed at the donor-acceptor interface. Experimental evidence show that this CT state has an energy lower than the bandgap of both the donor and the acceptor materials.[8,2,3] Two routes for populating the CT states have been reported. The first is by relaxation from singlet states formed via either above-bandgap excitation or injection from contacts.[9,10] Here the charge pair migrates to a donor-acceptor interface and minimizes its energy by populating the CT state at the interface. The second route for populating a CT complex is by direct optical excitation using sub-bandgap light.[11,12] Besides providing a recombination channel for Coulombically bound electron-hole pairs at donor-acceptor interfaces, there is also evidence of charge generation via the CT state. In regioregular- (rr) poly (3-hexylthiophene):[6,6]-phenyl-C_{61}-butyric acid methyl ester (P3HT:PCBM) a substantial number of sub-bandgap generated charges escape from the interface and can contribute to the solar cell photocurrent.[11,13] The CT state is also shown to be closely linked to the open circuit voltage of bulk heterojunction solar cells.[13]

The main obstacle for materials with low dielectric constants (and consequently a large r_c) to be operational in efficient solar cells is avoiding geminate recombination of the Coulombically bound charge pairs. The carrier generation in homogeneous polymeric semiconductors is of Onsager-type, which means that the generation is governed by the Brownian motion of the geminate pair within their mutual Coulomb potential. The criterion for this process is that the hopping distance is much shorter than the Coulomb radius. If a geminate pair can separate this distance, the probability for escaping the geminate

H. Aarnio, M. Nyman, Prof. R. Österbacka
Center for Functional Materials
Department for Natural Sciences
Åbo Akademi University
Porthansgatan 3, FI-20500, Turku, Finland
E-mail: rosterba@abo.fi
P. Sehati, Dr. S. Braun, Prof. M. Fahlman
Department of Physics
Chemistry and Biology
Linköping University
58183 Linköping, Sweden
Prof. M. P. de Jong
MESA+ Institute for Nanotechnology
University of Twente
7500 AE Enschede, The Netherlands

DOI: 10.1002/aenm.201100074

recombination is exactly one half and the carriers become free to participate in the transport. When an electric field is applied, the mutually attractive Coulomb potential will be lowered leading to a decreased Coulomb radius and consequently the carrier generation will show field dependence.

It has been shown that the recombination rate of charges is a good measure of the suitability of a solar cell blend.[14] Compared to the normal Langevin recombination (the time reversal of Onsager generation) in homogeneous materials, good solar cells made from rr-P3HT:PCBM blends show up to four orders of magnitude lower recombination rates, depending on the thermal treatment.[15] The reason for the low recombination coefficient is still not clarified. Given that this reduced recombination is a key to the success of the rr-P3HT:PCBM blend, further examination of the charge dissociation and recombination process in this system is called for.

In this communication we propose that thermal treatment will cause energetic shifts of polaron states at the P3HT:PCBM interfaces, causing spontaneous charge transfer and dipole formation at the interfaces. We show ultraviolet photoelectron spectroscopy (UPS) results on both regiorandom- (rra) and rr-P3HT before, during and after heat treatment, from which we obtain estimates of the positively charged polaron energies at the interface as well as in the bulk and how they depend on the thermal history and regioregularity. Finally, we present steady state photoinduced absorption (PA) spectroscopy measurements on rra- and rr-P3HT:PCBM films, using both above- and below-gap excitation light, and discuss how annealing, the lamellar structure and the interfacial dipoles affect generation and lifetimes of free charges.

To clarify the effect of annealing on the electronic structure and film morphology of rr- and regiorandom- (rra) P3HT, ultraviolet photoelectron spectroscopy (UPS) measurements were performed on both rr- and rra-P3HT thin films on Au (further details are provided in the Experimental section), see **Table 1**, and the results interpreted by the so-called Integer Charge Transfer (ICT) model.[16–18] The vertical ionization potential (IP) obtained by the UPS technique includes the inter- and intra-molecular electronic relaxation that occurs in response to the creation of a hole in a molecular orbital and thus captures the electronic part of the polaronic relaxation energy in π-conjugated materials as well as the screening of the surrounding medium. Tracking changes in film morphology by following the evolution of the UPS-derived IP is thus a viable method that has been employed previously on alkyl-substituted polythiophenes,[19–21] as e.g. better packing of the polythiophene chains will lead to better intermolecular screening and hence lower IP. Note that the UPS-derived IP represents the average vertical ionization potential of the material in the probed region and hence does not yield information on the local order at a buried interface. Furthermore, the IP does not include the geometrical relaxation of the material in response to the created hole, so the true polaronic formation energy where both the electronic and geometric relaxation has been included is not obtained. The ICT model can be used in combination with UPS data, however, to determine the energy of the positive (negative) integer charge transfer states E_{ICT+} (E_{ICT-}),[17,18,16] defined as the lowest energy required to take away one electron (highest energy gained from adding one electron) from (to) the molecule/polymer at an interface producing a fully relaxed state, i.e., polarons in π-conjugated molecules and polymers, see **Figure 1**. Note that both electronic and geometrical relaxation

Table 1. Results from UPS measurements on rra- and rr-P3HT. The positive integer charge transfer level, E_{ICT+}, vertical ionization potential, IP, and the energy difference between IP and E_{ICT+}, VBE, measured by UPS for the pristine films at RT, elevated temperatures and after cooling to RT, all done in situ. Experimental error ±0.05 eV.

rra-P3HT	Pristine sample, RT	50 °C	80 °C	110 °C	150 °C	RT
E_{ICT+} [eV]	4.30	4.30	4.30	4.25	4.05	4.05
IP [eV]	4.70	4.65	4.75	5.05	5.20	4.75
VBE [eV]	0.40	0.35	0.45	0.80	1.15	0.70
rr-P3HT	Pristine sample, RT	50 °C	80 °C	110 °C	150 °C	RT
E_{ICT+} [eV]	4.40	4.40	4.35	4.25	4.05	4.00
IP [eV]	4.50	4.50	4.50	4.50	4.50	4.45
VBE [eV]	0.10	0.10	0.15	0.25	0.45	0.45

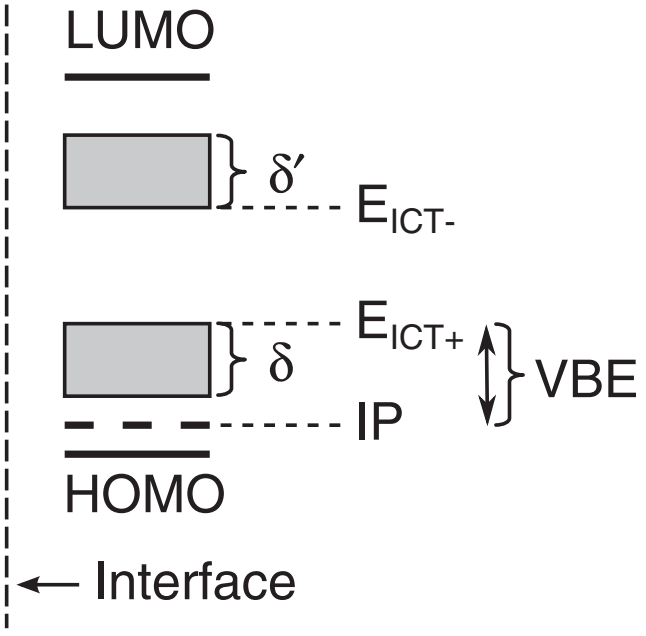

Figure 1. Energy level diagram of a π-conjugated molecule/polymer at an interface. The Highest Occupied Molecular Orbital (HOMO) and Lowest Unoccupied Molecular Orbital (LUMO) of the neutral system are shown as solid black lines. The fully relaxed integer charge transfer states (polarons in the case of polymers) that are created upon oxidation or reduction of the molecule/polymer at the interface are drawn in the gap. Just as in the bulk of the organic films, the energy of charge carrying states formed upon oxidation/reduction will have a Gaussian distribution with a width (δ, δ' in the figure) that depends on inter- and intra-molecular order, ring torsion, local screening, etc. The highest lying oxidized state and the lowest lying reduced states at the interface define the position of the E_{ICT+} and E_{ICT-}, respectively. The vertical ionization potential (IP) is indicated by the thick dashed line. Depending on the size of the energy related to bond reorganization as compared to the energetic disorder (δ), the UPS-measured IP may or may not lie within the polaron density of states. VBE is defined as the energy difference between the UPS-derived IP and E_{ICT+}.

are included in the E_{ICT+} and E_{ICT-}, as well as Coulombic interaction with the opposite "mirroring" charge on the substrate and dielectric screening from neighboring molecules, effects of intrinsic dipoles, etc.,[16,17,22,23,18] and thus contain information about the local order at that interface, which may differ from the bulk. The energy difference between IP and E_{ICT+}, is referred to as VBE (vertical binding energy) in this paper, see Figure 1.

We observe that pristine rra-P3HT, which forms a disordered film, has a pinning energy E_{ICT+} = 4.3 eV (equivalent to the upper edge of the positively charged polaron energetic distribution in rra-P3HT at the interface) and a vertical ionization potential (IP) of 4.7 eV. As the film temperature is elevated, we see that the IP increases substantially at T = 110 °C and reaches a maximum of 5.20 eV at T = 150 °C. Cooling the films to room temperature (RT) reduces the IP value to 4.75 eV. Coupled to the increase in IP, we see a decrease in E_{ICT+} also occurring at T = 110 °C and reaching a minimum of 4.05 eV at T = 150 °C. Subsequent cooling to RT does not change the E_{ICT+} value, which remains at 4.05 eV. The temperature-dependent evolution of the rr-P3HT films is quite different. Pristine rr-P3HT, which shows a lamellar structure, has a pinning energy E_{ICT+} = 4.4 eV and an IP of 4.5 eV. As the film temperature is elevated, we see no increase in IP while post-annealing cooling of the films to RT reduces the IP value marginally to 4.45 eV. We do see a decrease in E_{ICT+} occurring at T = 110 °C and reaching a minimum of 4.05 eV at T = 150 °C, just as for rra-P3HT. Subsequent cooling to RT decreases the E_{ICT+} marginally to 4.00 eV.

Thermal cycling of the PCBM from RT to 150 °C to RT yields a decrease in the E_{ICT-} level down to ~4.1 eV from the 4.2 to 4.4 eV values reported for pristine PCBM.[23,24] This might be due to a change in morphology, or a purification effect as a result of the heating. The quadrupole effect might also affect the results if the order at the interface between the Al oxide substrate used in this case and the PCBM is increased after the thermal cycling.[25] To clarify this, further studies on the PCBM are called for, but are beyond the scope of this article.

Using the ICT model, we interpret the results as follows. The comparatively large IP of 4.7 eV and VBE of 0.4 eV for pristine rra-P3HT indicate localized polarons, which is expected due to both inter- and intrachain disorder in the films. The increase in IP seen upon high temperatures is assigned to a decrease of the π-conjugation length due to increased inter-ring torsion and hence an increase of the band gap, the well-known thermochromism effect in alkyl-substituted polythiophenes.[26,19,27] The decrease in E_{ICT+} is indicative of a decrease in π-conjugation length, as the polarons become confined to shorter segments of the polymer chains, increasing the local bond distortion and pushing the polaron states deeper into the gap in analogy to what has been demonstrated for poly(p-phenylenevinylene) derivatives.[28] As the samples are cooled back to RT and reach equilibrium, the IP is recovered as the inter chain torsion returns to the RT values as well as the pre-heating inter-chain packing. Not all chains return to their pristine form, however, as some chains retain their high temperature conformation.[19] These chains with their corresponding low E_{ICT+} values then dominate the interface interaction, as they represent the most easily oxidized sites at the interface, and the Fermi level for the post-annealing films then remains pinned at 4.05 eV, even though the majority of the chains in the film have returned to "normal".

The evolution of the rr-P3HT films differs significantly in comparison. For the pristine rr-P3HT films, we see a low IP of 4.5 eV and a very small VBE, less than 0.1 eV. The lower IP corresponds to longer intrachain π-conjugation length and better screening from neighboring chains as the interchain packing is superior in this case. The small VBE indicates that the polarons are well delocalized, possibly over several neighboring chains.[29,30] The UPS data thus show that the pristine rr-P3HT films are defined by excellent inter- and intrachain order, in the bulk as well as at the interface, as expected from literature where it is well known that rr-P3HT aggregates into a 2D lamellar structure.[4,31–33,29] Upon annealing, we see no increase in IP, in stark contrast to the behaviour of rra-P3HT. The explanation is found in the crystallinity of the rr-P3HT films, which prevents the chains inside of the grains from undergoing interring torsion as it would disrupt the tight π–π packing of the polymer chains: the chains are collectively locked in place. The chains at the edges of the grains, however, are comparatively free to move, and some of these chains undergo thermal-induced increases in inter-ring torsion and hence decreases in the π-conjugation length and interchain π–π interaction. These chains in turn dominate the interface energetics with the substrate and again the Fermi level gets pinned to these localized polaron states around 4.05 eV. Cooling to room temperature does not return all of these chains to their pristine conformation, so the Fermi level remains pinned to the lower value, even though the bulk polarons retain their delocalized nature, which is possibly even improved by an annealing-induced increase of the macroscopic order in the films as the IP is slightly lowered.

For P3HT:PCBM blends, these results suggest that annealing in both the rr-P3HT and rra-P3HT cases will create a charge transfer dipole at the P3HT:PCBM interface with the negative side of the dipole pointing into the PCBM acceptor layer, as annealing at 110 °C or above introduces chains at the interface with localized polarons and corresponding E_{ICT+} values low enough (4.05/4.0 eV for rra-/rr-P3HT, respectively) to promote spontaneous charge transfer to the PCBM (E_{ICT-} = 4.1 eV). Theoretical models predict that interfacial dipoles with this direction will enhance exciton dissociation into free charge carriers, significantly decreasing the chance that the electron and hole states become trapped at the interface by Coulomb forces where they eventually would recombine resulting in a loss of photocurrent.[25,34] Furthermore, the interfacial dipoles will populate the most easily oxidized polymer chains or chain segments on the P3HT side of the heterojunction (most likely to undergo structural relaxation), and the most easily reduced PCBM molecules at the other side, as noted earlier. In this way, the most tightly bound sites where charge transfer electron-hole pairs could be created at the interface are already occupied by interfacial dipoles in the (dark) ground state and are consequently not available to participate in the exciton dissociation process following a photon absorption event.[23] This ensures that the charge transfer states formed immediately upon exciton dissociation are slightly "hotter" than otherwise would be the case. Hot charge transfer states facilitate an increased chance of full separation and collection at the external contacts according to theoretical predictions,[35] so the annealed P3HT:PCBM combination offers a further advantage in this regard.

To show the effect of heat treatment on the steady state charge concentrations and lifetimes, we measure room temperature photoinduced absorption spectra of the P3HT:PCBM blends both before and after heat treatment. Photoinduced absorption probes the absorption caused by photogenerated species in the P3HT:PCBM blend alone, without electrical contacts present. Because interfacial CT states can be directly excited using sub-bandgap light, the CT states give us a tool for studying charge formation from low-energy excitons generated at the interfaces versus higher-energy excitons generated in the bulk of the blend. This is important, because heat treatment is typically associated with a segregation of the polymer and fullerene phases, reducing the interfacial area.[36] Consquently charge generation from the interface should be reduced after heat treatment, assuming that there are no qualitative changes to the interfaces.

Photoinduced absorption spectra for the pure rr- and rra-P3HT polymers have been studied in detail before.[29,37] Using above gap (514 nm) excitation, rra-P3HT shows a weak polaron absorption, but is dominated by a large absorption band at 1.1 eV that has previously been ascribed to triplet excitons.[29] Polaron absorption is characterized by two correlated absorption peaks P1 and P2 at low and high energy, respectively. In the lamellar structure, delocalized polarons appear with red- and blue shifted P1 and P2 peaks, respectively. In rr-P3HT only the absoption of delocalized polarons is observed.[29] Our results support this (not shown). Above-gap excitation of PCBM yielded negligible PA. Further, using sub-bandgap excitation light (785 nm), we found that there is no discernible sub-bandgap absorption in the PA measurements for rr-P3HT, and for rra-P3HT it is also negligible. Annealing does not change the PA spectra significantly. The bandgaps for rr-P3HT and rra-P3HT lie at ~1.9 eV and ~2.2 eV, respectively.

Upon mixing PCBM with rra-P3HT the PA spectrum changes character. There is no sign of triplet excitons anymore, and the spectral features upon 514 nm (above-bandgap) excitation are dominated by weak absorption from Coulombically bound localized polarons (**Figure 2**a). Direct excitation of the CT states with 785 nm (sub-bandgap) light produces a qualitatively similar excitation spectrum, albeit at even lower charge concentration (Figure 2b). Annealing does not have any significant effect on the spectra, with the exception of a small shift in the in-phase and out-of-phase components in the 514 nm excitation spectrum.

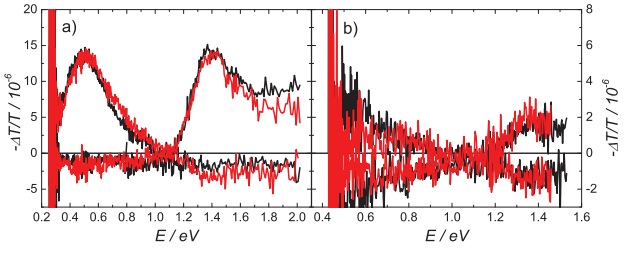

Figure 2. PA spectra of rra-P3HT:PCBM using a) 514 nm (2.41 eV) excitation light and b) 785 nm (1.58 eV) excitation light, measured at room temperature. Spectra before annealing are shown in black, and after annealing in red. In-phase signals are positive and quadrature signals negative.

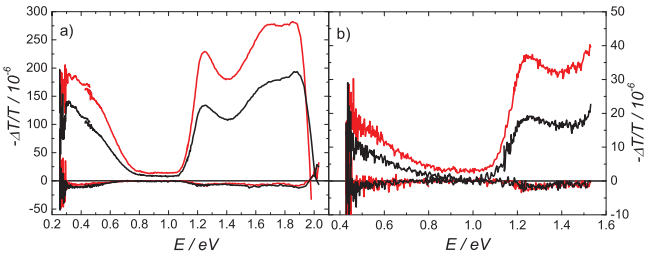

Figure 3. PA spectra of rr-P3HT:PCBM using a) 514 nm (2.41 eV) excitation light and b) 785 nm (1.58 eV) excitation light, measured at room temperature. Spectra before annealing are shown in black, and after annealing in red. In-phase signals are positive and quadrature signals negative.

Above-gap excitation on the rr-P3HT:PCBM blend generates more delocalized polarons (**Figure 3**a), as is expected for an ordered, efficient bulk heterojunction material. Even sub-bandgap excitation generates a substantial amount of delocalized polarons (Figure 3b), roughly seven times more in the steady state than in the rra-P3HT:PCBM blend. The PA spectra for above- and below-gap excitation are qualitatively similar. Annealing increases the PA amplitude for this blend by roughly a factor of two using both excitation wavelengths, and the in-phase/out-of-phase ratios change somewhat. There is also evidence of a slight improvement in the 2D lamellar structure upon annealing, visible in the above-gap spectrum in the form of a more pronounced delocalized polaron transition at ~1.7 eV. This has been attributed to increased crystallinity of P3HT,[29,30] and is in agreement with the slight lowering of the IP observed in the UPS measurements.

Lifetimes of the polarons are estimated from the ratio between the in-phase and quadrature components of the PA spectra, assuming nondispersive recombination.[38] Steady state charge concentrations (n) are estimated from the high energy polaron absorption peak amplitudes of the PA spectra, using $PA = n\sigma d$, where $\sigma = 10^{-16}$ cm^2 is the assumed absorption cross-section, and d is the thickness of the film or $d = \alpha_L^{-1}$ (where α_L is the absorption coefficient of the film for the excitation wavelength), whichever is smaller. The values for the lifetimes and charge densities as determined from PA data are presented in **Table 2**.

There is a clear difference in lifetimes of the polarons when comparing below- and above-bandgap excitation, with below-bandgap absorption yielding longer lifetimes. This is in accordance with the above-bandgap generated charges being "hotter", and thus having more energy to either escape the interface and finding non-geminate (second order) recombination sites (in rr-P3HT:PCBM) or populating less confined sites close to the interface and thus having an increased chance for recombining geminately (rra-P3HT:PCBM). Polarons in rra-P3HT:PCBM are also generally much more longer lived than those in rr-P3HT:PCBM caused by the localized nature of the as-spun rra-P3HT compared to the rr-P3HT.

Heat treatment of rra-P3HT:PCBM does not increase the polaron concentration generated by above-bandgap light, but the lifetime of the polarons is somewhat increased. There are no significant changes in either charge concentration or lifetimes after heat treatment using sub-bandgap light.

Table 2. Lifetimes and charge concentrations extracted from photoinduced absorption spectroscopy data. Values for the lifetime τ and charge concentration n are given for 785 and 514 nm excitation wavelengths. The values are measured at 1.4 eV and 1.25 eV probe energies (on top of the polaron P2 absorption peak) for rra-P3HT:PCBM and rr-P3HT:PCBM, respectively. The error margins given are estimated from the noise in the data.

	Rra-P3HT:PCBM		Rr-P3HT:PCBM	
	Unannealed	Annealed	Unannealed	Annealed
τ_{785} [μs]	1000(±300)	900(±300)	90(±30)	60(±20)
τ_{514} [μs]	170(±50)	280(±50)	70(±10)	35(±5)
n_{785} [cm^{-3}]	$0.7(\pm0.1)\times10^{15}$	$0.9(\pm0.1)\times10^{15}$	$0.46(\pm0.01)\times10^{16}$	$0.90(\pm0.01)\times10^{16}$
n_{514} [cm^{-3}]	$4.8(\pm0.1)\times10^{15}$	$4.8(\pm0.1)\times10^{15}$	$14.9(\pm0.02)\times10^{16}$	$25.5(\pm0.02)\times10^{16}$

Heat treatment of the rr-P3HT:PCBM blend shows similar results both using above- and below-bandgap excitation. Charge concentrations increase significantly after heat treatment, and at the same time the lifetimes are significantly reduced. This is expected, because intensity dependence measurements (not shown) indicate that we are operating in a regime with bimolecular (non-geminate) recombination.

The suggested interfacial dipole formation in the P3HT:PCBM blends from the UPS results is supported quite well by the PA results. The lack of changes in the charge concentrations in the rra-P3HT:PCBM blend upon heat treatment is a consequence of the disordered nature of the blend, which is largely unaffected by the heat treatment. The small increase in the polaron lifetime after heat treatment using above-bandgap excitation could be due to small morphological changes such as PCBM aggregation, but can also be explained by hindered geminate recombination of the localized charge pairs, caused by dipole formation at the interfaces.[34]

The results for the rr-P3HT:PCBM blend are more interesting. In this material the lamellar structure of the rr-P3HT allows for efficient delocalization and high mobility of the polarons. Charges can escape fairly well from the interfaces already before heat treatment, but we propose that introduction of interfacial dipoles by heat treatment makes this escape process much more efficient, resulting in the observed higher steady state charge concentration. This increase in charge concentration can also be explained using morphological arguments, as it is well known that heat treatment of a P3HT:PCBM blend results in a phase separation of the components, and thus the likelihood for electrons and holes to meet and recombine during transport is reduced.[36] The results with sub-bandgap excitation of the rr-P3HT:PCBM blend, however, can not be explained by morphological arguments. The total amount of interfaces in the bulk is reduced due to demixing of the rr-P3HT and PCBM components following heat treatment. Since sub-bandgap excitation can only happen at interfaces where wave functions of the donor and acceptor overlap and form inter-bandgap ground state CT states, we expect that the sub-bandgap PA in the case of rr-P3HT:PCBM should be reduced after heat treatment. Instead we observe an increase in the sub-bandgap generated charges from the interfaces, which indicates a significant improvement of the charge generation capability of the interface. This could be in part due to an increased density of ground state CT states at the interface, but since these are likely to also work as recombination channels, and the second order recombination in heat treated films (compared to untreated) is shown to be reduced,[15] we find it unlikely that this alone could explain the improved charge generation. Thus we suggest that the reason for increased charge generation from the CT states is the formation of interfacial dipoles as suggested by the UPS data.

In conclusion, we present UPS measurements on rr- and rra-P3HT, and show using the ICT model that heat treatment of P3HT:PCBM blends promotes spontaneous charge transfer from the positive integer charge transfer state E_{ICT+} of P3HT to the negative ICT state E_{ICT-} of PCBM. We show that the resulting dipole formation at the interface between P3HT and PCBM can inhibit charge recombination at the interfaces, and in the ordered rr-P3HT:PCBM blend promote dissociation of Coulombically bound polaron pairs away from the interface into delocalized polarons. The UPS and ICT model results are verified by PA measurements on both rra- and rr-P3HT:PCBM blends, before and after heat treatment. Sub-bandgap generated polarons show longer lifetimes as compared to above-bandgap generated charges in both rr-P3HT:PCBM and rra-P3HT:PCBM blends due to their lower energy forcing them to populate more relaxed states. The rr-P3HT:PCBM blend shows superior polaron generation, which is further improved by annealing, and shorter lifetimes compared to the rra-P3HT:PCBM blend, as expected from the lamellar ordering of rr-P3HT and the annealing-induced dipole formation at the interface. An increase of the sub-bandgap generated polarons in rr-P3HT:PCBM after annealing, when the amount of interfaces should be reduced, is a strong indication of enhanced charge pair dissociation efficiency of the interface. We attribute this to the interfacial dipoles. The UPS/ICT and PA results are in good agreement with each other and offer in the dipole formation a plausible explanation as to why recombination in the rr-P3HT:PCBM blend is reduced.

Experimental Section

Photoinduced absorption spectroscopy: Samples were prepared from chlorobenzene solutions (60 mg ml^{-1}) of polymer:PCBM in 1:1 ratio by weight, by spincoating on sapphire substrates. The materials used were regioregular-P3HT (Plextronics OS2100), regiorandom-P3HT (Rieke) and PCBM (Solenne). Film thicknesses were 410 nm and 297 nm for the regioregular- and regiorandom-P3HT:PCBM films, respectively. Sample preparations were carried out in Nitrogen atmosphere. Annealing of the samples was performed on a hotplate at 120 °C for 15 minutes in Nitrogen atmosphere. For measurements, the sample was transferred to a cryostat (Janis Research), where it was kept under vacuum at room temperature (300 K). Photoinduced absorption was measured using

either an Argon ion laser (Coherent Innova) for 514 nm excitation light, or a diode laser (Power Technology) for 785 nm excitation light. Both were set to an excitation intensity of 180 mW cm^{-2}. The excitation light was modulated by a mechanical chopper at 133 Hz. A tungsten projector lamp with appropriate cutoff filters served as probe light, which, after passing through the sample, was directed through a monochromator (Acton Research Corporation) and detected with Si, Ge and InSb detectors and a lock-in amplifier (Stanford Research).

We would like to point out that it has been shown that the CT state in P3HT:PCBM absorbs light with energy as low as 1 eV,[39,11,3,13] and therefore our probe light is constantly generating a background of charges of an unknown concentration. This can potentially lead to an underestimation in the values for the lifetimes (due to bimolecular recombination) and PA signal (due to ground state bleaching) presented in this article.

Ultraviolet photoelectron spectroscopy: The materials used were regioregular P3HT (Plextronics OS2100), regiorandom P3HT (Rieke) and PCBM (Solenne). Polycrystalline gold samples were cleaned ex-situ in a solution of ($5H_2O$, $1NH_4OH$ and $1H_2O_2$) at 85 °C for 5–10 min, yielding substrate work functions (typically 4.95 ± 0.1 eV) large enough to bring the rr- and rra-P3HT/metal interfaces into the positive pinning regime,[17] thereby allowing the determination of the positive integer charge transfer level E_{ICT+},[16] of the polymers. Thin films of rr- and rra-P3HT were subsequently spin-coated from dichlorobenzene solutions onto the cleaned Au substrates. The samples were measured in an UHV photoelectron spectrometer with a base pressure of 10^{-10} mbar, using monochromatized HeI photons ($h\nu$ = 21.2 eV) with a binding energy resolution of ±0.05 eV. The heating and cooling of the samples were carried out in situ at better than 10^{-10} mbar. Temperature control was maintained throughout the measurement series using a PID regulator. PCBM samples were spin-coated from dichlorobenzene solutions unto a variety of different substrates so that the work function range allowed for the determination of the negative integer charge transfer state E_{ICT-}.[17] The work function of the organic-on-gold films were obtained from the secondary electron tail using the standard procedure.[17] The vertical ionization potential of the polymer films were obtained using the position of leading edge of the frontier occupied feature in the HeI spectra.[17]

Acknowledgements

This work is partly financed via the Morphoso project, Academy of Finland projects 116995 and 135262 and via the Swedish Research Council (project grant 2007-4245).

Received: February 17, 2011
Revised: May 29, 2011
Published online:

[1] G. Yu, J. Gao, J. C. Hummelen, F. Wudl, A. J. Heeger, *Science* **1995**, *270*, 1789.
[2] M. Hallerman, I. Kriegel, E. Da Como, J. M. Berger, E. von Hauff, J. Feldmann, *Adv. Funct. Mater.* **2009**, *19*, 3662.
[3] D. Veldman, S. C. J. Meskers, R. A. J. Janssen, *Adv. Funct. Mater.* **2009**, *19*, 1939.
[4] H. Sirringhaus, P. J. Brown, R. H. Friend, M. M. Nielsen, K. Bechgaard, B. M. W. Langeveld-Voss, A. J. H. Spiering, R. A. J. Janssen, E. W. Meijer, P. Herwig, D. M. de Leeuw, *Nature* **1999**, *401*, 685.
[5] J.-L. Brédas, J. E. Norton, J. Cornil, V. Coropceanu, *Acc. Chem. Res.* **2009**, *42*, 1691.
[6] T. Liu, A. Troisi, *J. Phys. Chem. C* **2011**, *115*, 2406.
[7] C. F. N. Marchiori, M. Koehler, *Synt. Met.* **2010**, *160*, 643.
[8] W. Osikowicz, M. P. de Jong, W. R. Salaneck, *Adv. Mater.* **2007**, *19*, 4213.
[9] K. Tvingstedt, K. Vandewal, A. Gadisa, F. Zhang, J. Manca, O. Inganäs, *J. Am. Chem. Soc.* **2009**, *131*, 11819.
[10] D. Veldman, Ö. Ipec, S. C. J. Meskers, J. Sweelssen, M. M. Koetse, S. C. Veenstra, J. M. Kroon, S. S. van Bavel, J. Loos, R. A. J. Janssen, *J. Am. Chem. Soc.* **2008**, *130*, 7721.
[11] K. Vandewal, A. Gadisa, W. D. Oosterbaan, S. Bertho, F. Banishoeib, I. Van Severen, L. Lutsen, T. J. Cleij, D. Vanderzande, J. V. Manca, *Adv. Funct. Mater.* **2008**, *18*, 2064.
[12] T. Drori, C.-X. Sheng, A. Ndobe, S. Singh, J. Holt, Z. V. Vardeny, *Phys. Rev. Lett.* **2008**, *101*, 037401.
[13] K. Vandewal, K. Tvingstedt, A. Gadisa, O. Inganäs, J. V. Manca, *Nature Mater.* **2009**, *8*, 904.
[14] A. Pivrikas, G. Juška, A. J. Mozer, M. Scharber, K. Arlauskas, N. S. Sariciftci, H. Stubb, R. Österbacka, *Phys. Rev. Lett.* **2005**, *94*, 176806.
[15] R. Österbacka, A. Pivrikas, G. Juška, A. Poškus, H. Aarnio, G. Sliaužys, K. Genevičius, K. Arlauskas, N. S. Sariciftci, *IEEE J. Sel. Topics Quantum Electron.* **2010**, *16*, 1738.
[16] S. Braun, W. R. Salaneck, M. Fahlman, *Adv. Mater.* **2009**, *21*, 1450.
[17] C. Tengstedt, W. Osikowicz, W. R. Salaneck, I. D. Parker, C.-H. Hsu, M. Fahlman, *Appl. Phys. Lett.* **2006**, *88*, 053502.
[18] M. Fahlman, A. Crispin, X. Crispin, S. K. M. Henze, M. P. de Jong, W. Osikowicz, C. Tengstedt, W. R. Salaneck, *J. Phys. Condens. Matter* **2007**, *19*, 183202.
[19] W. R. Salaneck, O. Inganäs, B. Thémans, J. O. Nilsson, B. Sjögren, J.-E. Österholm, J. L. Brédas, S. Svensson, *J. Chem. Phys.* **1988**, *89*, 4613.
[20] K. Kanai, T. Miyazaki, H. Suzuki, M. Inaba, Y. Ouchi, K. Seki, *Phys. Chem. Chem. Phys.* **2010**, *12*, 273.
[21] K. Kanai, T. Miyazaki, T. Wakita, K. Akaike, T. Yokoya, Y. Ouchi, K. Seki, *Adv. Funct. Mater.* **2010**, *20*, 2046.
[22] J. C. Blakesley, N. C. Greenham, *J. Appl. Phys.* **2009**, *106*, 034507.
[23] P. Sehati, S. Braun, L. Lindell, X. Liu, L. M. Andersson, M. Fahlman, *IEEE J. Sel. Topics Quantum Electron.* **2010**, *16*, 1718.
[24] R. J. Davis, M. T. Lloyd, S. R. Ferreira, M. J. Bruzek, S. E. Watkins, L. Lindell, P. Sehati, M. Fahlman, J. E. Anthony, J. W. P. Hsu, *J. Mater. Chem.* **2011**, *21*, 1721.
[25] S. Verlaak, D. Beljonne, D. Cheyns, C. Rolin, M. Linares, F. Castet, J. Cornil, P. Heremans, *Adv. Funct. Mater.* **2009**, *19*, 3809.
[26] S. Rughooputh, S. Hotta, A. J. Heeger, F. Wudl, *J. Polym. Sci., Part B: Polym. Phys.* **1987**, *25*, 1071.
[27] M. Ahlskog, J. Paloheimo, H. Stubb, P. Dyreklev, M. Fahlman, O. Inganäs, M. R. Andersson, *J. Appl. Phys.* **1994**, *76*, 893.
[28] M. Fahlman, P. Bröms, D. A. dos Santos, S. C. Moratti, N. Johansson, K. Xing, R. H. Friend, A. B. Holmes, J. L. Brédas, W. R. Salaneck, *J. Chem. Phys.* **1995**, *102*, 8167.
[29] R. Österbacka, C. P. An, X. M. Jiang, Z. V. Vardeny, *Science* **2000**, *287*, 839.
[30] D. Beljonne, J. Cornil, H. Sirringhaus, P. J. Brown, M. Shkunov, R. H. Friend, J.-L. Brédas, *Adv. Funct. Mater.* **2001**, *11*, 229.
[31] R. M. Beal, A. Stavrinadis, J. H. Warner, J. M. Smith, H. E. Assender, A. A. R. Watt, *Macromolecules* **2010**, *43*, 2343.
[32] R. D. McCullough, S. Tristram-Nagle, S. P. Williams, R. D. Lowe, M. Jayaraman, *J. Am. Chem. Soc.* **1993**, *115*, 4910.
[33] T.-A. Chen, X. Wu, R. D. Rieke, *J. Am. Chem. Soc.* **1995**, *117*, 233.
[34] V. I. Arkhipov, P. Heremans, H. Bässler, *Appl. Phys. Lett.* **2003**, *82*, 4605.
[35] B. Kippelen, J.-L. Brédas, *Energy Environ. Sci.* **2009**, *2*, 251.
[36] X. Yang, J. Loos, S. C. Veenstra, W. J. H. Verhees, M. M. Wienk, J. M. Kroon, M. A. J. Michels, R. A. J. Janssen, *Nano Lett.* **2005**, *5*, 579.
[37] X. M. Jiang, R. Österbacka, O. Korovyanko, C. P. An, B. Horowitz, R. A. J. Janssen, Z. V. Vardeny, *Adv. Funct. Mater.* **2002**, *12*, 587.
[38] H. Aarnio, M. Westerling, R. Österbacka, M. Svensson, M. R. Andersson, H. Stubb, *Chem. Phys.* **2006**, *321*, 127.
[39] L. Goris, A. Poruba, L. Hod'ákova, M. Vaněček, K. Haenen, M. Nesládek, P. Wagner, D. Vanderzande, L. De Schepper, J. V. Manca, *Appl. Phys. Lett.* **2006**, *88*, 052113.